Retinal Image Vessel Width Analysis in Retinopathy of Prematurity

R. Manjunatha[1*] and H. S. Sheshadri[2]
[1]Assistant Professor, [2]Professor
[1&2]Department of Electronics and Communication Engineering, P.E.S. College of Engineering, Mandya, Karnataka, India
*Corresponding Author
E-Mail: rmanjunatha@gmail.com

Abstract - **This paper aims at development of Oscillating Pendulum Based Algorithm (OPBA) for retinal image width computation and analysis for the investigation of Retinopathy of prematurity (ROP). The algorithms have been explained in detail with theoretical investigations and simulations, images from local hospital data base were considered in the investigation. Further this paper also presents an overview of direct retinal vessel width computation method along with the comparative analysis. The results obtained are found to be encouraging for analysis of plus disease under ROP.**
Keywords: **DVW, OPBA, Retinal Vessel, Retinopathy, ROP**

I. INTRODUCTION

The retinal vessel tortuosity and dilatation are important factors of diagnosis for ROP and ROP plus disease [9]. Retinal images contain great details of retinal arteries, veins and optical disk information. The morphological characters of the veins and arteries have been studied by the practicing ophthalmologists for diagnosis of retinal diseases like, Cataracts, Glaucoma, Strabismus, Coloboma, Diabetic retinopathy, Hypertensive retinopathy etc. With the advantage of computer vision and image processing technologies the problem of retinal image analysis has been studied extensively with the outcome of novel ideas and algorithms focusing on retinal vessel width and tortuosity measurements.

Faraz Oloumi *et al.,* [3] presented Gabour filter based MTA tracking and width measurement, where in the width is measured as two times the boundary distance, accuracy of which depends on distance mapping. Luo Gang *et al.,* [2] presented second order Gaussian filter for vessel detection based on the intensity level changes in binary image using Gaussian function estimating vessel profiles for width calculations, similarly Clare M. Wilson *et al.,* [7] introduced standard deviation of the Gaussian profile with maximum-likelihood fitting model to estimate the width. Alauddin Bhuiyan *et al.,* [1] presented a rotating mask based vessel width measurement procedure, where in they employed texture based classifier with Gabor filter for vessel center line and edge extraction, to which they applied the rotating mask. A similar approach was employed by *C*. Heneghan *et al.,* [5] and Stabingis *et al.,* [4]. These approaches limit the accuracy of vessel width measurement as they lack to address localization of the vessel information with running slope. Problem of localization can be resolved by measuring differential curvature over local segments of a vessel with

dynamic segment length. This paper presents an account of a novel method, developed elsewhere [10] in comparison to the in place width computation with quantitative analysis. Contents of the discussion starts with short details of pre-processing of retinal image in section II, followed with overview of methods in section III. Finally the outcome of analytical experimentation of the methods is presented in section IV with related tables and details.

II. PRE-PROCESSING

The retinal image (RI) is pre-processed to make it ready for width analysis. The fundus images obtained by the Retcam is converted from RGB into gray scale (GI) image followed by AHE and binarization (BI) with dynamic threshold D_{th} (refer equation 1), details of the process are discussed elsewhere [3], [6]. Fig.1 (a) shows the retinal image M-32, from the local data and Fig. 1(b) is the binarized version of M-32.
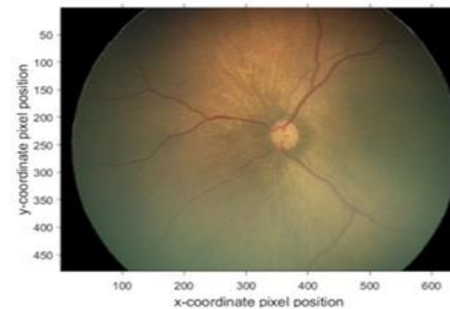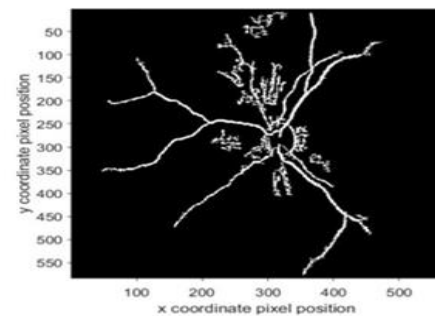

Fig. 1 a) Fundus RI

Fig. 1 b) Binarized RI

$$BI = \begin{cases} 1 & if \quad GI(x,y) \geq D_{th} \\ 0 & otherwise \end{cases} \text{-------------------}1$$

III. VESSEL WIDTH CALCULATIONS

Binarized form of retinal image is taken for width computation then from the binarized skeleton largest circle fits inside white pixels region, the average of all that circles that is calculated as a width of that image, presented by Sivakumar *et al.,* [8]. In this work employed two methods to measure the vessel width in pre-processed retinal image. First method is simple in place computation method with computation efficiency while suffering through width in accuracies to be discussed in results section. Second method is computationally demanding compared to the first one, still performs better in comparison to the methods cited and discussed in introduction at the same time offering considerable accuracy. Following paragraphs presents the snippets of the methods.

A. Direct pixel-to-pixel computation (DVW).
B. Oscillating Pendulum Based Algorithm (OPBA) computation.

A. *Direct Pixel-To-Pixel Computation:* In the method of direct computation the width of the vessel is computed as an average parameter over the length of the vessel. Where in width at sample point is computed in place by considering pixel in opposite boundaries of the vessel (UB-Upper boundary and LB- Lower boundary), x axis pixel coordinate positions are x1,x2,x3…..xn and y axis pixel coordinate positions are varying with two levels y_{min} and y_{max}. The width will be w1,w2,w3……wn. Where w1=$(y1_{max} - y1_{min})$, w2= $(y2_{max}-y2_{min})$ …… wn=$(yn_{max} -yn_{min})$,as shown in Fig.2 a) In this method, there will be an error because of geometrical orientation of a vessel to overcome this one more approach is presented here is OPBA computation (RVW). To compute the segment and vessel average by equations 5 and 6 [10].
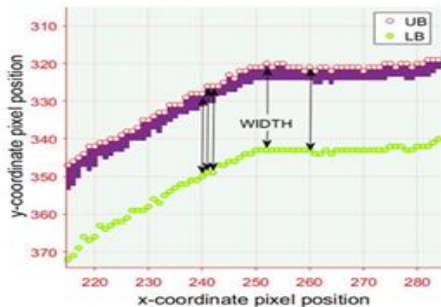

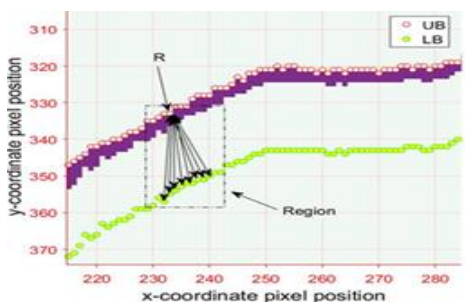
Fig. 2 a) Direct pixel-to-pixel computation (DVW)

Fig. 2 b) OPBA computation

B. OPBA Computation: The process of major vessel extraction and segmentation along with boundary extraction is followed as was discussed in method (A), for measuring width at any pixel with OPBA was applied. Segment size is selected based on the slop variation and length of the vessel, so as to have adequate accuracy in width measurement. In OPBA a region of appropriate width was selected for slope free width computation. The OPBA results are normalized with segment and vessel averaging as per equations 5 and 6 [10]. In OPBA the upper boundary fix a reference point R, from this find the widths about 16 pixels both sides from that reference point and minimum value of this is the vessel width of that reference point. Example reference point R at (x30, y_{max} 30), the widths will be w1= (y_{max}30, y_{min}23), w2= (y_{max}30, y_{min}24) ….. w16= (y_{max}30, y_{min}38) is as shown in Fig. 2b. To compute the segment and vessel average by equations 5 and 6 [10].

IV. MAJOR VESSEL EXTRACTION

The vessel width is computed considering longer major vessel [6], [10]. A statistical approach as discussed in [6], [10], is applied to extract the major vessels. Depending on the RI a number of major vessels V_{Mi} are identified as shown in Fig. 3b.The extracted major vessels shows random angular orientation which should be theta θ compensated for further processing, the major vessel V1 from Fig.3a which is angle compensated by value theta is as shown in Fig. 3b.

$$V_{Mi} = \{V_{S1}, V_{S2}, V_{S3}.....V_{SN}\}$$ ----------------- (2)

$$\theta_M = \{\theta_{M1}, \theta_{M2}, \theta_{M3}.....\theta_{Mn}\}$$ ------------------ (3)

Where θ_M the angle of major vessels and n is is the vessel number.
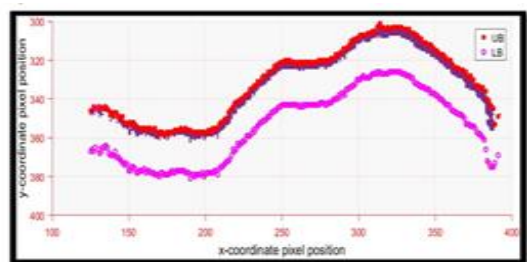

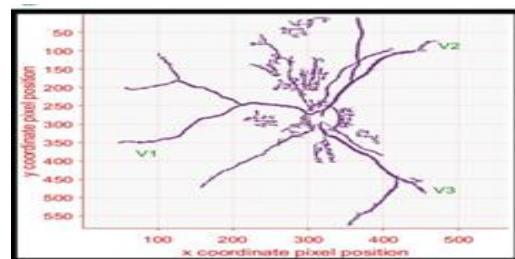Fig. 3 a) Major vessel V1 from Fig. 2b, with offset of 20 pixels for visibility

Fig. 3 b) Vasculature of RI (Image M-32 from local data set)

With the special distribution of the vessels, the width is estimated as average effective width of the vessel, $w_{V_{mi}}$ rather than a single point of measure. Each of the major

vessels of length LV_{Mi} is divided into 8 segments of length LS_j, equation (4) is for the ith major vessel.

$$LS_j = \frac{LV_{Mi}}{8} \text{------------------ (4)}$$

In every segment width is measured at each pixel site of the vessel, with labels W1, W2 etc. representing width measured at reference points 1 and 2 in etc. As pointed earlier length of segment is set selected based on the overall vessel length, so as to reduce the width error due statistical variations. For every j^{th} segment one average width, $\tilde{w}_{V_{mi},S_j}$ is computed, with S_j number of segments resulting in S_j number of average widths per vessel, refer equation (5).

$$\tilde{w}_{V_{mi},S_j} = \frac{\sum_{n=1}^{S_{s,V_{mi}}} w_n}{S_{s,V_{mi}}} \text{ ------------------ (5)}$$

Where S_s is segment size

$$w_{V_{mi}} = \frac{\sum_{j=1}^{M_{V_{mi}}} \tilde{w}_{V_{mi},S_j}}{N_{V_{mi}}} \text{ ------------------ (6)}$$

Consequently the segment width averages are normalized with respect to number of segments yielding effective vessel width, equation (6).

V. RESULTS AND DISCUSSION

The preprocessed retinal images are operated by the major vessel extraction function to identify and extract the major vessels. The major vessels thus identified are processed further to extract the boundaries of the vessels, these vessels with identified boundaries are individually taken through the width computation algorithms DVW and OPBA. Fig. 4 (a), (b) shows the two retinal images of different cases, selected from local data base as based on discussions with ophthalmologists.
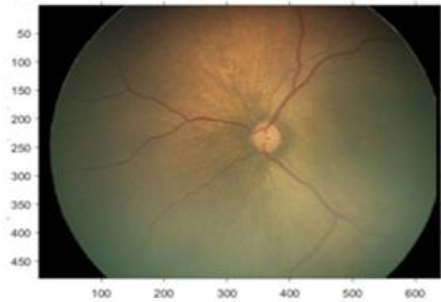

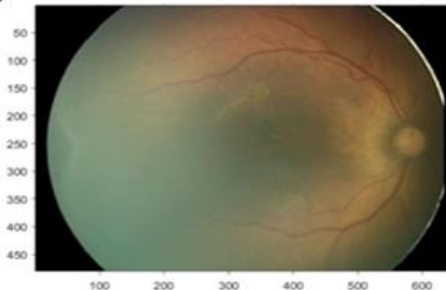Fig. 4 a) Retinal image M-32 from local data set
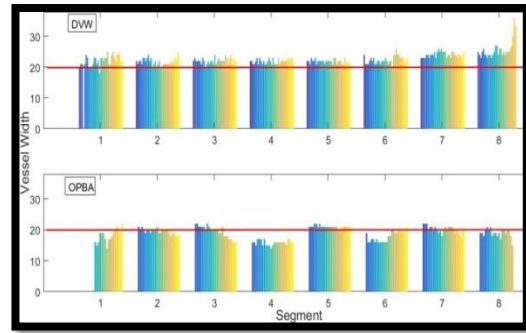

Fig. 4 b) Retinal image M-13 from local data set

Fig. 5 Comparative results of DVW vs OPBA

As discussed in section II every vessel is divided into 8 segments and width is computed at every pixel of the segment, while considering the pixels in the upper boundary as reference for the OPBA regions. Fig.5 shows the statistics of the two algorithm outcomes for major vessel V1 of M-32. Observation of the bars on one side shows a remarkable difference in segment 8 measurements, with DVW width exceeding 20 by considerable margin, on the side OPBA results for the same segment shows more prominent results with width of around 20. This variation in results is due to the running slope of the vessel in segment 8, OPBA compensated for the running slop with region wise operation whereas the DVW failed.
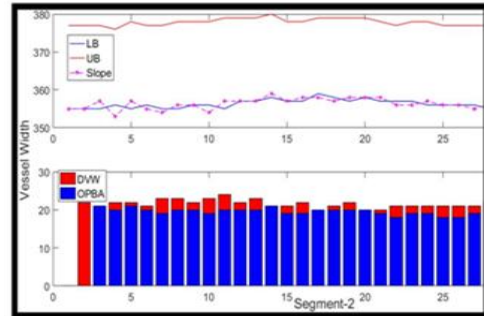

Fig. 6 a) Results of comparison for vessel V1 at segment 2
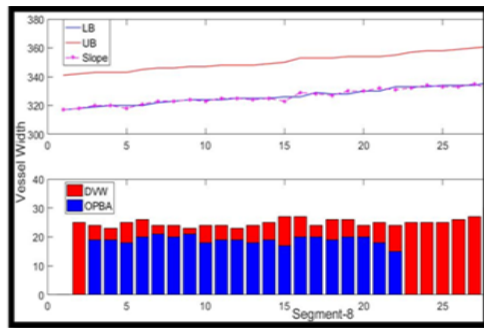
Fig. 6 b) Results of comparison for vessel V1 at segment 8

Further Fig. 6 shows the insight view for the segments 2 and 8, segment 2 is having flat running whereas segment shows running slope this makes the in place computation applied by DVW to fail in predicting the width. The accuracy offered by OPBA is found to be function of region width and segment length, these parameters must be selected appropriately to have optimal width results.

Table I shows the list of segment wise and average vessel width measurements obtained for the image M-32 of local data base. The measurements are obtained by applying DVW and OPBA, here in 3 vessels are identified as major vessels, V1, V2 and V3 with vessel lengths 266,245 and 225 each of the three vessels are processed individually for the width calculation. The measurements corresponding to the vessel 1 shows normal impression excluding segment 7 and segment 8, the results of this exhibits a drastic rise in width due to the slope of the vessel in these segments. As pointed out earlier, the extent of drastic variation is considerably high in method 1, as witnessed in segment 8 of the segment wise width bar chart in Fig.5 and 6a. This is compensated in method 2 by adopting the segment size and region width as shown in Fig.5 and 6b. Highlighted figures in the tables, shows the strength of OPBA in computing vessel width with better accuracy in spite of segment wise running slope. The average vessel width computed by OPBA are more consistent compared to the DVW.

TABLE I SEGMENT WISE AND AVERAGE VESSEL WIDTH MEASUREMENTS OBTAINED FOR THE IMAGE M-32

	Seg. No.	$\tilde{w}_{V_1,S_j}$		$\tilde{w}_{V_2,S_j}$		$\tilde{w}_{V_3,S_j}$	
		DVW	OPBA	DVW	OPBA	DVW	OPBA
Image M-32	1	2.1212	0.2963	3.0323	1.2400	6.2500	1.4545
	2	1.7576	0.5926	3.4194	2.2800	3.7143	2.3636
	3	2.0909	0.7778	3.8387	2.6000	3.7857	2.3636
	4	1.9091	0.2963	3.0000	2.2800	3.6786	2.6364
Avg. width at each segment level	5	1.8485	1.1111	3.4516	2.2400	4.1786	2.0909
	6	2.3636	0.6296	3.9032	2.1600	4.1786	2.0909
	7	4.0909	2.5556	4.1935	2.2000	3.5714	2.2273
	8	4.9697	1.7778	1.9677	0.6000	3.1786	1.2273
Avg. vessel width ($w_{V_{mi}}$)		2.64	1.00	3.35	1.95	4.06	2.05

Table II shows the list of segment wise and average vessel width measurements obtained for the image M-13 of local data base. The measurements are obtained by applying DVW and OPBA, here in 4 vessels are identified as major vessels, V1, V2,V3 and V4 with vessel lengths 319,345,323 and 197 each of the three vessels are processed individually for the width calculation. In this case also it is observed that sudden rise in the width variations due to slope of the vessel, very high variation segment average results can be neglected for the average vessel calculations. Highlighted figures show the differences between DVW and OPBA algorithms. Glancing through the Table I and II it can be inferred with OPBA that the maximum vessel width in M32 is 2.05 and DVW is 4.06, where as in M-13 it is 4.18 with OPBA and 8.23 in DVW. The variation in results indicates the effect of method employed in vessel width measurement, though in this case here DVW appears to help in identifying the abnormal image, however there are chances that DVW may end up with wrong diagnostic results with large variation between normal and abnormal RI vessel widths. The OPBA results exhibits consistency in width analysis in terms of average width.

TABLE II SEGMENT WISE AND AVERAGE VESSEL WIDTH MEASUREMENTS OBTAINED FOR THE IMAGE M-13

	Seg. No.	$\tilde{w}_{V_1,S_j}$		$\tilde{w}_{V_2,S_j}$		$\tilde{w}_{V_3,S_j}$		$\tilde{w}_{V_4,S_j}$	
		DVW	OPBA	DVW	OPBA	DVW	OPBA	DVW	OPBA
Image M-13	1	3.8250	1.3529	5.6047	3.2432	4.6500	1.7353	9.8000	1.2105
	2	2.5250	1.2941	2.7907	1.4865	5.8750	2.5588	2.5600	1.0000
	3	3.3750	1.9118	7.1860	5.4054	6.7250	4.5000	3.9200	2.2632
	4	3.5750	1.8824	4.3721	1.7297	4.5750	2.2353	3.2400	0.5263
Avg. width at each segment level	5	3.0250	1.3235	6.6047	2.6757	4.2250	2.8235	2.1200	0.4737
	6	4.5500	2.7059	11.8140	10.1081	3.3250	1.5588	3.6000	1.3158
	7	7.0250	4.8235	9.5814	4.2703	4.3750	1.8824	1.6400	1.0000
	8	90.2250	77.5294	17.9535	4.5405	6.5750	2.6765	1.1200	0.1579
Avg. vessel width ($w_{V_{mi}}$)		3.98	2.18	8.23	4.18	5.04	2.49	3.5	0.99

VI. CONCLUSION

The results of DVW and OPBA algorithms are found to be in agreement for the flat running vessels. OPBA is found to be effective in vessels with running slope, where DVW computations are inconsistent and slope affected. Though in some cases DVW appears to help in identifying the retinal images with vessels having abnormal width; however there are chances that DVW may end up with wrong diagnostic results with large variation between normal and abnormal RI vessel widths. The OPBA results exhibits consistency in width analysis in terms of average width. OPBA results accuracy can be improvised by compensating each segment orientation and segment size.

ACKNOWLEDGEMENT

REFERENCES

[1] Alauddin Bhuiyan, Baikunth Nath, Joselíto J. Chua, and Kotagiri Ramamohanarao "An Efficient Method for Vessel Width Measurement on Color Retinal Images" *Biosignals*, 178-185, 2008.

[2] Luo Gang, Opas Chutatape, and Shankar M. Krishnan "Detection and Measurement of Retinal Vessels in Fundus Images Using Amplitude Modified Second-Order Gaussian Filter" *IEEE Transactions on Biomedical Engineering*, Vol. 49, No. 2, February 2002.

[3] Faraz Oloumi, Rangaraj M. Rangayyan, and Anna L. Ells "Measurement of Vessel Width in Retinal Fundus Images of Preterm Infants with Plus Disease", *IEEE International Symposium on Medical Measurements and Applications (MeMeA)-2014*.

[4] GiedriusStabingis *et al.,* "Automatization of Eye Fundus Vessel Width Measurements" DOI: 10.1007/978-3-319-68195-5_85, vipima ge-2017, *Springer International Publishing,* published in 2018.

[5] C. Heneghan, J. Flynn, M. O'Keefe, and M. Cahill, "Characterization of changes in blood vessels width and tortuosity in retinopathy of prematurity using image analysis," *Medical Image Analysis*, Vol. 6, No. 1, pp. 407–429, 2002.

[6] R Manjunatha, Mahesh Koti and Dr. H.S. Sheshadri "Boundary Extraction and Tortuosity Calculation in Retinal Fundus Images" *Springer, ICERECT-2018, PESCE, Mandya.*

[7] Clare M. Wilson *et al.,* "Computerized Analysis of Retinal Vessel Width and Tortuosity in Premature Infant" *Investigative Ophthalmology & Visual Science,* Vol. 49, No. 8, DOI: 10.1167/iovs.07-135August 2008.

[8] R. Sivakumar, Manu Eldho, C.V. Jiji, Anand Vineka, and Renu John "Diagnosis of Plus Diseases for the Automated Screening of Retinopathy of Prematurity in Preterm Infants" *International Conference on Industrial and Information Systems (ICIIS)-2016*.

[9] Michael F. Chiang *et al.,* "Plus Disease In Retinopathy of Prematurity: An Analysis of Diagnostic Performance" *Trans Am Ophthalmol Soc*., Vol. 105, 2007

[10] R. Manjunatha and H. S. Sheshadri "Boundary Extraction and Vessel width Calculation in Retinal Fundus Images" *Asian Journal of Engineering and Applied Technology,* Vol. 8, No. 2, 2019.